

# Solar-Wind based intelligent battery controller in distributed generation system using ANFIS controller

<sup>1</sup>P. Shashavali, <sup>2</sup>N. Rajesh Kumar Gowd, <sup>3</sup>Bukke Harinadha Nayak

<sup>1&2</sup> Assistant Professor, Department of EEE, S.K. University College of Engg. and Tech., Ananthapuramu, Andhra Pradesh,

<sup>3</sup>M.Tech Student, Dept. of EEE, Sri Krishnadevaraya University, Ananthapuramu, Andhra Pradesh.

**Abstract:** Now-a-days, the generation of electricity is done with the renewable energy sources. But the main problem with these renewable energy sources is their intermittent nature. As single renewable energy resource is used, the reliability of the power system is decreased. In order to vanquish the problem, storage system with large capacity should be used. But this increases the size as well as the cost of the system which drastically reduces the flexibility. To overcome this problem a standalone hybrid power supply system is designed by integrating the solar and wind energy to generate electricity. The hybrid system increases the generation capacity without increasing the storage unit and maintains reliable electricity to the consumer. The proposed system has been modeled using MATLAB/Simulink and verify under variable sources and load condition without compromising with the power quality issue.

*IndexTerms:* Renewable energy, Solar, Wind, MPPT, Hybrid Power quality, Adaptive Neuro-Fuzzy Inference System (ANFIS).

## I. INTRODUCTION

Increased demand of energy throughout the world, shortage of fossil fuels and environmental problems caused by conventional power generation has led to an urgent search for renewable energy sources. Renewable Energy is the energy that comes from natural resources such as sunlight, wind, tides and geothermal heat which are naturally replenished at a constant rate. Renewable Energy sources are clean, inexhaustible and are thought to free energy sources, such as solar and wind energies. Over the past few years, renewable energies represent a rapidly growing share of total energy supply, including heat and transportation. A standalone distributed generation system is effective for electrifying a remote rural area where traditional grid connection is absent. Due to the absence of the grid connectivity the battery maintains the reliability of the supplied electricity. The battery is used to store the energy when the renewable sources are available and this stored energy is utilized whenever energy is to be supplied to the consumers. The present study is addressing a new technology to integrate the generated electricity from solar and wind energy sources in a standalone distributed generation system to ensure optimum reliability to the consumer.

## II. Proposed configuration

The proposed configuration of a standalone hybrid power supply system (SHPPS) is shown in Fig. 1. In this proposed system, both the solar energy and the wind energy is converted to electrical energy using PV array and a wind turbine generator (WTG) set. An incremental conductance (IC) based maximum power point tracking (MPPT) controller is attached to the PV array to maintain the power at the maximum power level during variable solar irradiance and then, the obtained energy is supplied to the battery bank. For WTG the optimum torque controlled (OTC) based MPPT controller is maintaining the maximum power level under variable wind speed. To store the generated AC from the WTG a three phase rectifier unit is attached to the system which converts generated AC to DC and then, the obtained energy is supplied to the battery bank. In this proposed system to store the generated energy from solar and wind, individual battery bank is connected to the individual sources separately and the generated energy is supplied to the load using a hybrid battery management system. The charge controller maintains the battery management system in such a way that a single battery unit is in operation at a time and the other remains in standby condition.

The voltage of the operating battery is increased using stepped up DC-DC converter and further converted to AC with the desired quality using a ANFIS controlled DC-AC inverter to maintain desired voltage.

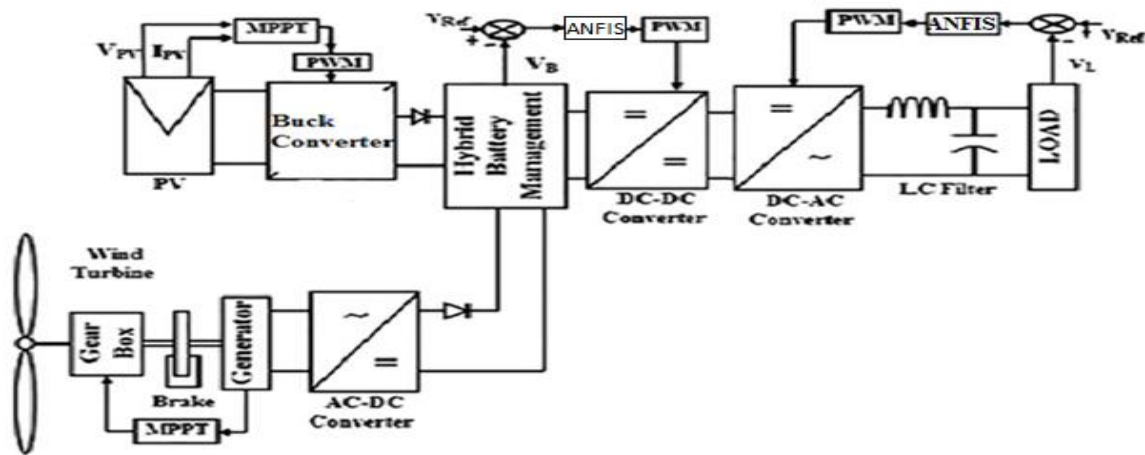


Fig. 1. A standalone hybrid power supply system using solar and wind energy.

### 2. 1. Photovoltaic cell circuit diagram and performance:

The solar irradiance is directly converted to electricity using photovoltaic (PV) cell. In a PV characteristic there are basically three important points viz. open circuit voltage, short circuit current and maximum power point. The maximum power that can be extracted from a PV cell are at the maximum power points. Usually manufacturers provide these parameters in their data sheets for a particular PV cell or module. A PV model using the data of Sun Power E20/435 W has been built in MATLAB Simulation software. To maintain the generated voltage at the maximum power level a buck converter is utilized here operated by the incremental conductance (IC) based MPPT controller. In a buck converter the semiconductor switch continuously turns ON and OFF by the switching signals provided by the MPPT controller to maintain the desired output voltage at the maximum level. When thyristor is turned ON, the output voltage is same as the input voltage and if it is turned OFF, the output voltage is zero. If this diode is absent, a high induced EMF in inductance may cause damage to the switching device. The inductor and capacitor are applied here to maintain the current and voltage ripple within the limit. The output voltage of the buck converter is

$$V_{out} = DV_{in} \dots(1)$$

where,  $V_{in}$  is the input voltage of the Buck converter,  $V_{out}$  is the output voltage of the buck converter and  $D$  represents the duty cycle. The I-V and P-V characteristic of the array are shown in Figs. 2 and 3 considering the temperature of the environment is Constant.

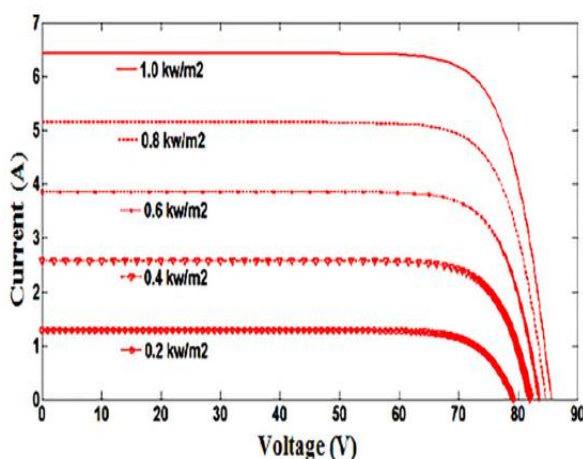


Fig. 2. I-V curve of PV array.

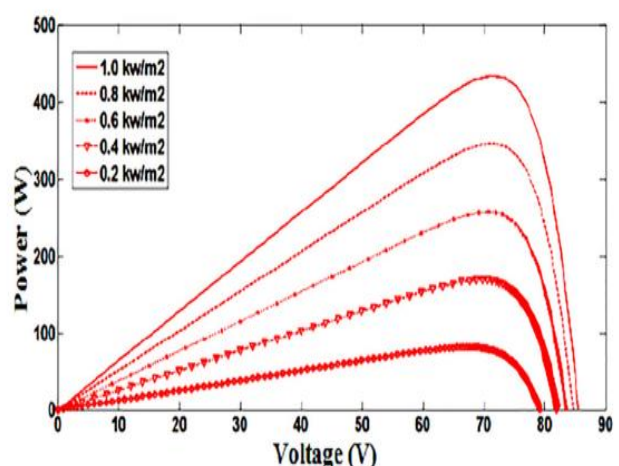


Fig. 3. P-V curve of PV array.

## 2.2. Incremental conductance (IC) method

In this proposed system to extract power under variable irradiance of the sun the incremental conductance (IC) based MPPT controller is used here. To obtain maximum power the voltage and the current is observed and the conductance of the network is analyzed. The maximum power is obtain by changing the duty cycle of the controller and by maintain desired voltage. The driving equation of the IC based MPPT method is

$$\frac{dP}{dV} = \frac{d(VI)}{dV} = I + V \frac{dI}{dV} = 0 \quad \dots(2)$$

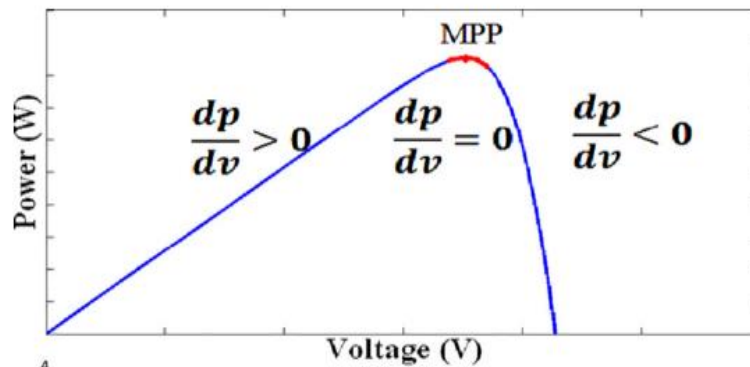


Fig. 4. Operating power (P) and voltage (V) curve of the conventional IC algorithm.

In Fig. 4 indicates the voltage and power profile of a PV array under a constant solar irradiance. Due to variation of voltage the extracting power also changes. The PV array provides the maximum power when  $dp/dv=0$ . From the figure if the operating voltage of the PV array is less than the maximum power condition voltage the Eq. (2) modifies to

$$\frac{dI}{dV} > -\frac{I}{V}; \left( \frac{dP}{dV} > 0 \right) \quad \dots(3)$$

which indicates the less power drawn by the PV array with less voltage. But whenever the operating voltage is too high the PV array again draws less amount of power and the Eq. (2) modifies to

$$\frac{dI}{dV} < -\frac{I}{V}; \left( \frac{dP}{dV} < 0 \right) \quad \dots(4)$$

The Eq. (3) indicates left hand side of the maximum power condition and Eq. (4) satisfies the right hand side of the MPP condition observed in Fig. 4. The algorithm related to IC based MPPT controller is shown in Fig. 5. Where  $k$  represents the counter and  $D$  represents the duty cycle which operates the connected DC to DC converter to maintain the maximum power condition. During operation the duty cycle, is simultaneously changed to obtain the MPP condition at different irradiance as well as temperature under variable load condition also. Here, the counter senses the present voltage  $V(k)$  and  $I(k)$  and compute the conductance. Based on the measured conductance the duty cycle changes to reach the MPP based on the network conductance indicated in Eqs. (2)–(4).

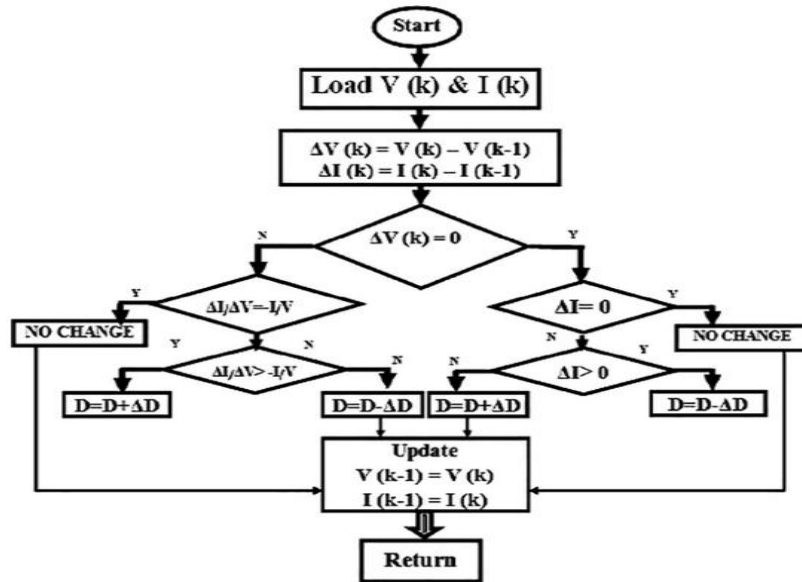


Fig. 5. Incremental Conductance (IC) algorithm for MPPT controller.

**2.3. Power generation using wind turbine:**

Wind Turbine (WT) converts the wind energy to the mechanical torque, which rotates the shaft of an electrical generator to generate electrical energy. Wind comes from atmospheric changes: changes in temperature and pressure makes the air move around the surface of the earth. All of which is triggered by the sun. So in a way, wind energy is another form of solar power. A wind turbine captures the wind, which then produces a renewable energy source. The wind makes the rotor spin; as the rotor spins, the movement of the blades drives a generator that creates energy. The motion of the blades turning is kinetic energy. It is this power that we convert into electricity. The power generated by the wind turbine is

$$P_w = 0.5C_p(\lambda, \beta) \times (V_w)^3 \dots(5)$$

where P is air density (kilograms per cubic meter); Vx, wind speed in meters per second; A, blades' swept area; Cp, turbine-rotor power coefficient; λ, tip-speed ratio; β, pitch angle.

The maximum power is found using maximum power point tracking algorithm (MPPT) is used to capture maximum energy from the fluctuating wind speed. And the tip-speed ratio is defined as

$$\lambda = \frac{\omega_r}{V_w} \dots(6)$$

where, ω<sub>r</sub> is the angular velocity of rotor [rad/s], R is the rotor radius [m] and V<sub>w</sub> is the wind speed upstream of the rotor [m/s].

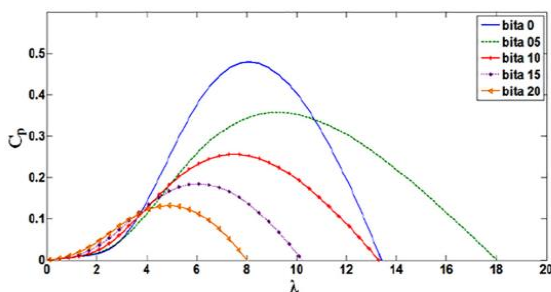


Fig. 6. Analytical approximation of Cp (λ,β) characteristics.

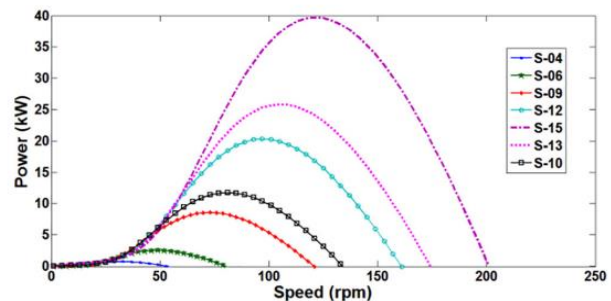


Fig. 7. Electrical power generated by the turbine as a function of the rotor speed for different wind speeds.

The Cp-λ characteristics, for different values of the pitch angle b, are illustrated in Fig. 6 From the characteristic of Cp-λ it is evident that the maximum value of turbine-rotor-power coefficient (Cp) is achieved for β = 0. The profile of the power of the wind turbine is depends on the turbine speed which is shown in Fig. 7.

### III. ANFIS CONTROLLER:

An adaptive neuro-fuzzy inference system or adaptive network-based fuzzy inference system (ANFIS) is a kind of artificial neural network that is based on Takagi–Sugeno fuzzy inference system. Since it integrates both neural networks and fuzzy logic principles, it has potential to capture the benefits of both in a single framework. Its inference system corresponds to a set of fuzzy IF–THEN rules that have learning capability to approximate nonlinear functions. Hence, ANFIS is considered to be a universal estimator. For using the ANFIS in a more efficient and optimal way, one can use the best parameters obtained by genetic algorithm.

#### ANFIS Architecture: Representing Takagi-Sugeno Fuzzy Model

For simplicity, we assume that the fuzzy inference system under consideration has two inputs  $x$  and  $y$  and one output  $z$ . For a first-order Takagi-Sugeno fuzzy model, a common rule set with two fuzzy if-then rules is the following:

Rule 1: If  $x$  is  $A_1$  and  $y$  is  $B_1$ , then  $f_1 = p_1x + q_1y + r_1$ ;

Rule 2: If  $x$  is  $A_2$  and  $y$  is  $B_2$ , then  $f_2 = p_2x + q_2y + r_2$ ;

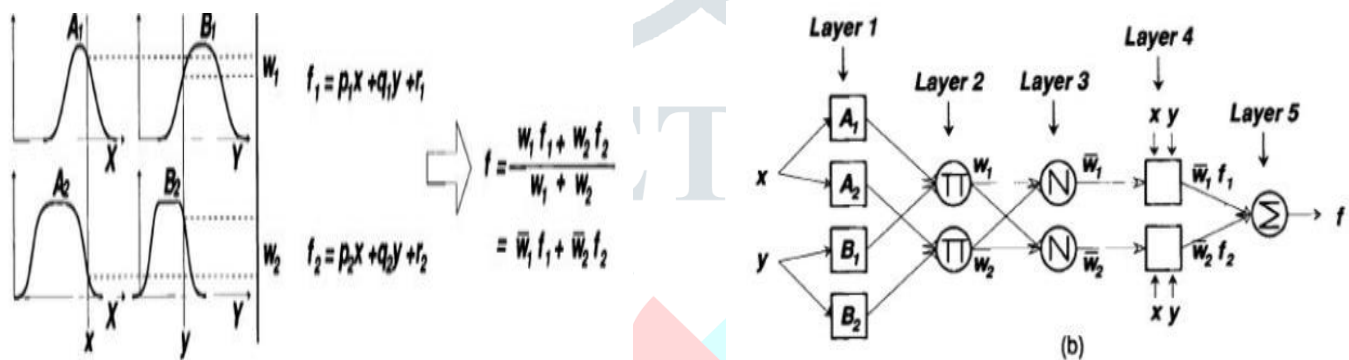


Figure 8(a) illustrates the reasoning mechanism for this Takagi-Sugeno model; the corresponding equivalent ANFIS architecture is as shown in Figure 8(b), where nodes of the same layer have similar functions, as described next. (Here we denote the output of the  $i^{th}$  node in layer 1 as  $O_i$ ,  $i$ .

**Layer 1** Every node  $i$  in this layer is an adaptive node with a node function

$$O_i^1 = \mu_{A_i}(x)$$

where  $x$  (or  $y$ ) is the input to node  $i$  and  $A_i$  (or  $B_i$ ) is a linguistic label (such as "small" or "large") associated with this node. In other words,  $O_i$  is the membership grade of a fuzzy set  $A$  ( $=A_1, A_2, B_1$  or  $B_2$ ) and it specifies the degree to which the given input  $x$  (or  $y$ ) satisfies the quantifier  $A$ .

$$\mu_A(x) = \frac{1}{1 + |x - c_{ai}|^{2b}}, \mu_A(x) = \frac{1}{1 + |x - c_{ai}|^{2b}}$$

where  $\{a_i, b_i, c_i\}$  is the parameter set. As the values of these parameters change, the bell-shaped function varies accordingly, thus exhibiting various forms of membership function for fuzzy set  $A$ . Parameters in this layer are referred to as premise parameters.

**Layer 2** Every node in this layer is a fixed node labeled ANFIS, whose output is the product of all the incoming signals:

$$O_i^2 = w_i = \mu_{A_i}(x) \times \mu_{B_i}(y), \quad i = 1, 2$$

Each node output represents the firing strength of a rule. In general, any other T-norm operators that perform fuzzy AND can be used as the node function in this layer.

**Layer 3** Every node in this layer is a fixed node labeled N. The  $i$ th node calculates the ratio of the  $i$ th rule's firing strength to the sum of all rules' firing strengths:

$$O_i^3 = \bar{w}_i = \frac{w_i}{w_1 + w_2}, \quad i = 1, 2$$

For convenience, outputs of this layer are called normalized firing strengthes.

**Layer 4** Every node  $i$  in this layer is an adaptive node with a node function:

$$O_i^4 = \bar{w}_i f_i = \bar{w}_i (p_i x + q_i y + r_i), \quad i = 1, 2$$

where ANFIS is a normalized firing strength from layer 3 and  $\{p_i, q_i, r_i\}$  is the parameter set of this node. Parameters in this layer are referred to as consequent parameters.

**Layer 5** The single node in this layer is a fixed node labeled ANFIS, which computes the overall output as the summation of all incoming signals:

$$O_i^5 = \text{overall output} = \sum_i \bar{w}_i f_i = \frac{\sum_i w_i f_i}{\sum_i w_i}$$

Thus we have constructed an adaptive network that is functionally equivalent to a Sugeno fuzzy model.

### 3.1. Mathematical equation of PMSM

The generator model is implemented entirely in dq-coordinates. It means that there are no AC-states in the model. The generator is modelled with DC voltages and currents in a rotor-fixed rotating coordinate system which is illustrated in Figure. The equations for the d-axis and q-axis currents are defined as

$$\frac{di_{sd}}{dt} = -\frac{R_{sa}}{L_{sd}} i_{sd} + \omega_s \frac{L_{sq}}{L_{sd}} i_{sq} + \frac{1}{L_{sd}} u_{sd} \dots\dots(7)$$

$$\frac{di_{sq}}{dt} = -\frac{R_{sa}}{L_{sq}} i_{sq} - \omega_s \left( \frac{L_{sd}}{L_{sq}} i_{sd} + \frac{1}{L_{sq}} \psi_p \right) + \frac{1}{L_{sq}} u_{sq} \dots\dots(8)$$

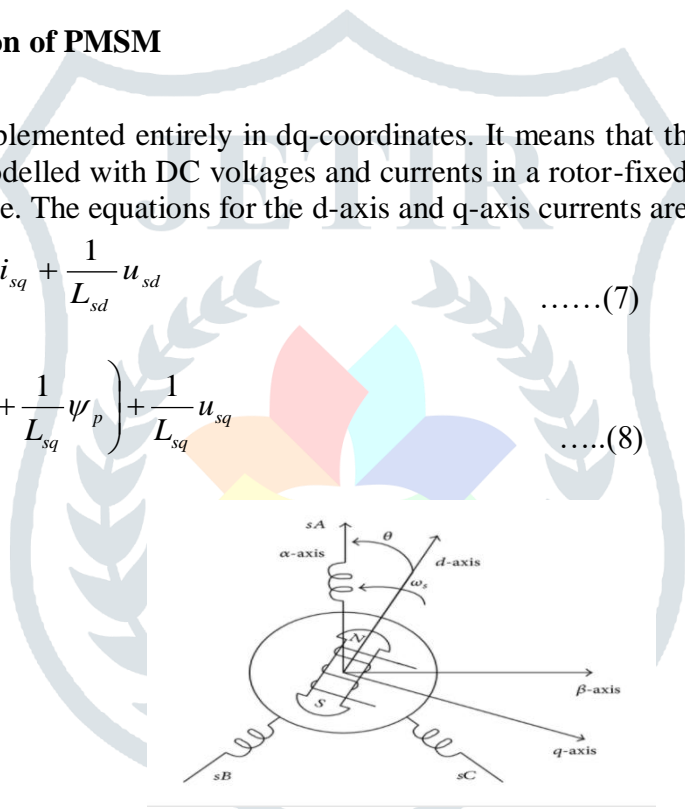


Fig-9 The dq-coordinate frame of the PMSG.

The power equation is given by:

$$P_{se} = \frac{3}{2} \left[ (R_s i_{sd}^2 + R_s i_{sq}^2) + L_s \left( \frac{d}{dt} i_{sd}^2 + \frac{d}{dt} i_{sq}^2 \right) + p \omega_m (\psi_{sd} - \psi_{sq} i_{sd}) \right] \dots\dots\dots(9)$$

The first term represents the power loss in the conductors, the second term indicates the time rate of change of storing energy in the magnetic fields and the third term express the energy conversion, from electrical energy to mechanical energy. From the third term can be express the electromagnetic torque because the power output from the motor shaft must be equal to the electromechanical power.

$$P_e = \omega_m T_e = \frac{3}{2} [ \omega_e \psi_{sd} i_{sq} - \omega_e \psi_{sq} i_{sd} ] \dots\dots(10)$$

The relation between the electrical velocity and the mechanical angular velocity of the motor depends on the number of pole pairs as presented below

$$\omega_e = p \omega_m \dots\dots(11)$$

$$\text{The torque is given by } T_e = \frac{3}{2} P [\varphi_m i_{sq} + (L_d - L_q) i_{sd} i_{sq}] \quad \dots(12)$$

In the final expression of the torque, Eq. (12), it can be observed that there are two terms, the first one represents the synchronous torque and is produced by the flux of the permanent magnets and the second term represents the reluctance torque and represents the torque produced by the difference of the inductances in dq reference frame. In the project the motor is surface mounted permanent magnet and in this case the inductances in dq reference frame are equal resulting a simpler expression of the electromagnetic torque, without the reluctance torque. With the assumption expressed above, the Eq. (14) has the following form

$$T_e = \frac{3}{2} P [\varphi_m i_{sq}] \quad \dots(13)$$

The mechanical equation of the machine is expressed as a function of the electromagnetic torque ( $T_e$ ), load torque ( $T_L$ ) and electrical velocity of the machine:

$$T_e = T_L + B \omega_m + J \frac{d\omega_m}{dt} \quad \dots(14)$$

where J is the moment of inertia and B is the viscous friction.

### 3.2. Optimal torque control (OTC):

For different speeds of wind turbine the generated torque is adjusted to its optimal value. If the conditions are optimal, based on Eq. (6), the optimum speed of the rotor can be estimated as

$$w_{m,opt} = \frac{v_w \lambda_{opt}}{R} = k_w v_w \quad \dots(15)$$

Combining Eqs. (5) and (15) yields the optimum mechanical power generated by the wind turbine is

$$P_{w,opt} = 0.5 C_p (\lambda, \beta) \times \left( \frac{R w_{opt}}{\lambda_{opt}} \right)^3 = k_{opt} (w_{m,opt}) \quad \dots(16)$$

Also the optimum torque calculated from the Eq. (17) is

$$T_{w,opt} = k_{opt} (w_{opt})^2 \quad \dots(17)$$

Optimal Torque control adjusts the generator torque to its optimal at different wind speeds. However, it requires the knowledge of turbine characteristics ( $C_{pmax}$  and  $\lambda_{opt}$ ). If the conditions are optimal, based on Eq. (17), the optimum speed of the rotor can be estimated as: Where  $K_{opt}$  is a constant determined by the wind turbine characteristics.

### 3.3. Performance of Battery and operation of charge controller:

The generic model of rechargeable battery has been used to get the better understanding and to study the performance of Battery connected hybrid system. The mathematical representation of charging and discharging of the lead acid battery is given by

$$V_{bat} = E_o - Ri - k \frac{Q}{it - 0.1Q} \cdot t^* - k \frac{Q}{Q - it} \cdot it + \exp(t)$$

$$V_{bat} = E_o - Ri - k \frac{Q}{Q - it} \cdot (it + t^*) + \exp(t) \quad \dots(18)$$

where  $V_{bat}$  represents battery voltage (V),  $E_0$  represents battery constant voltage (V),  $K$  represents polarization constant (V/(Ah)) or polarization resistance (X),  $Q$  represents battery capacity (Ah),  $i$  represents actual battery charge (Ah),  $A = \exp$  exponential zone amplitude (V),  $B = \exp$  exponential zone time constant inverse (Ah)<sup>-1</sup>,  $R$  represents internal resistance (X),  $i$  represents battery current (A),  $i^*$  represents filtered current (A).

For the Off grid distributed system, the charge controller design is less complicated for the single power source when compared to hybrid power sources based system. It is necessary to ensure required protection of the equipment and continuity of the energy flow. These two requirements are provided by the modified version of charge controller has been depicted in Fig. 8 where SPV and WTG are acting as a sources of electrical energy. The main problem arrives with the synchronization with the battery voltage due to different voltage the delivered energy circulating among the different sources.

Hence it is difficult to charge the battery using different energy sources. The solution for the problem of synchronization to the battery with two different energy sources in this case is to use two sets of battery bank. The WTG based secondary source has delivered the energy to increase the reliability of the power supply system without increasing the size of the battery bank. For the proposed system, there are two sources of energy in which the PV array acts as a primary source of energy. The charging and discharging of the battery mainly depends on the energy demand by the consumers and the energy generated by the sources. In the case of unavailability of solar energy, the battery connected to the primary sources is unable to provide energy. Then secondary sources provide the required energy to the consumer.

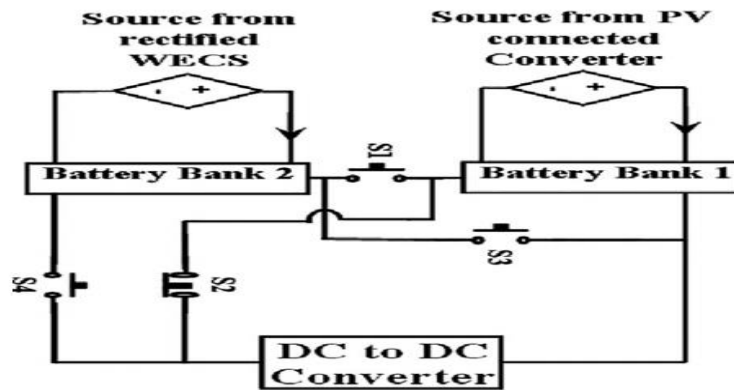


Fig. 10. Configuration of battery management for hybrid power supply system.

In the beginning, the values of the power level of the solar PV, the individual battery bank voltage and the SOC of the individual battery bank are measured and compared with a predefined value. In the initial stage, if the SOC of the battery and the generated power of the solar PV (SPV) is more than the reference value only switch S2 is ON and the battery bank 1 is connected to the load and the primary energy sources. If the generated energy by the SPV is less than the predefined value the switch S3 and S4 are ON and the battery bank 2 is connected to the load. Here also the energy supplied by the secondary energy source (WTG) to the battery is maintained the charging, discharging or in floating condition based on the supplied energy from the source to the battery bank 2 and the energy consumed by the load. In the worst condition whenever both of the individual sources are unavailable to provide adequate energy to the battery bank the SOC of the battery individually checked and if the SOC is low compared to the predefined value the battery voltage has also been checked. As the battery bank voltage is directly linked with SOC for minimum SOC condition the voltage of the individual battery bank is very low both of the battery banks are connected in series by switching on S1 and S4. If the SOC of the batteries is further reduced the battery bank is unable to maintain the required voltage and in that condition all the switches are in OFF condition and the load is thrown off. Here, during operation the charge controller maintains the hybrid system in a single source power supply system where either battery bank 1 or battery bank 2 is in operation. As the primary or the secondary sources of energy are always connected to the battery bank the generated energy is always transferred to the battery bank during standby condition also.

### 3.4. Boost converter:

In this chopper, the output voltage is always greater than input voltage and supplied to the inverter. Here also a switch is used, which is connected in parallel with the load. The stable high voltage obtained by the ANFIS controlled boost converter increase the stability of the generated voltage of the inverter unit. The output voltage obtained by the boost converter is

$$V_{out} = V_{in} \left( \frac{1}{1-D} \right) \quad \dots(19)$$

here,  $V_{in}$  is the input voltage of the Boost converter,  $V_{out}$  is the output voltage of the Boost converter,  $i_a$  is the average current at the load end,  $T$  is the cycle time period ( $T = 1/f_s$ ),  $f_s$  is the switching frequency,  $L$  is the selected inductor value,  $D$  is the Duty cycle.

**3.5. Three phase inverters:** The inverter is a device which converts DC to AC with the desired frequency. A three phase bridge type Voltage source inverter (VSI) converts generated DC into three phase AC. The three legs of the inverter circuit consist of two MOSFET switch operated by specially designed PWM signals. The Switches simultaneously ON and OFF using desired pulses obtained from pulse width

modulation technique to generate balanced three phase output voltages to supply a three phase load. The PWM technique consists of three sinusoidal modulating signals with appropriate 120° phase shift, generated by the vector control circuit is compared with high frequency triangular carrier signal and generates the required pulses for switching operation. The line-to-line RMS voltage at the fundamental frequency, due to 120° phase the displacement between phase voltages can be written as

$$V_{ph} = \left( \frac{2\sqrt{2}}{\Pi} \right) \cos\left( \frac{\Pi}{6} \right) \dots(20)$$

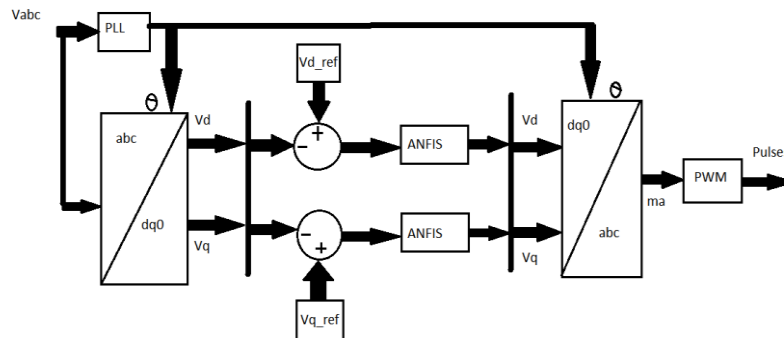
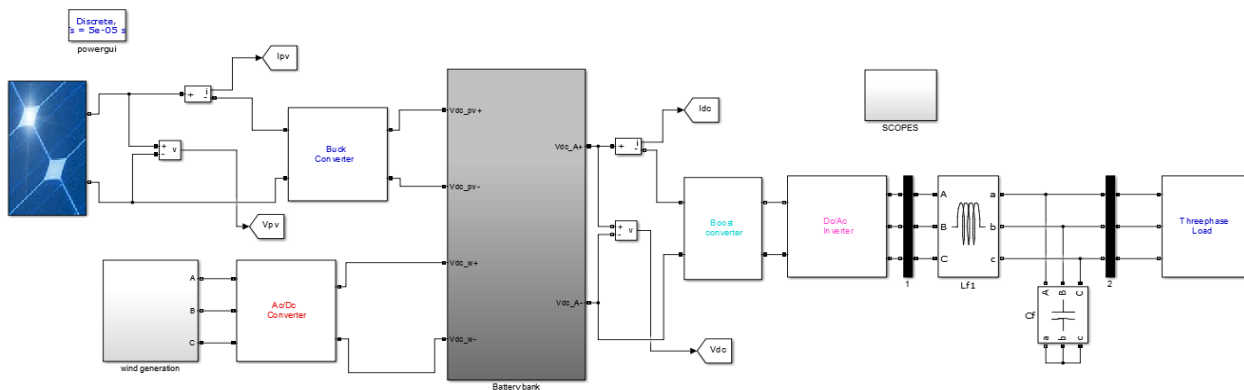


Fig. 11. Block diagram for ANFIS voltage regulator.

where  $V_{ph}$  is the obtained phase voltage at the terminals, and  $V_{dc}$  is the input voltage of the inverter. The PID control PWM technique is utilized to generate desired pulses for the inverter.

**IV. RESULT AND DISCUSSION:**

The photovoltaic system has been used as the primary source for the generation of electrical energy. This energy varies for different irradiance of the sun. To get the reliable operation and to maximize the generated voltage, a number of solar cells are connected in series along with the battery bank. The WECS is attached to the system as a secondary source of energy by which the generated energy increase without increasing the capacity of the battery banks. The generated electricity from the PV and the Wind are then connected to a battery unit which individually uses a charge controller, which maintains the charging, discharging and floating condition and also provides protection of the battery bank. To increase the voltage of the battery a ANFIS controlled boost converter is attached to the system.



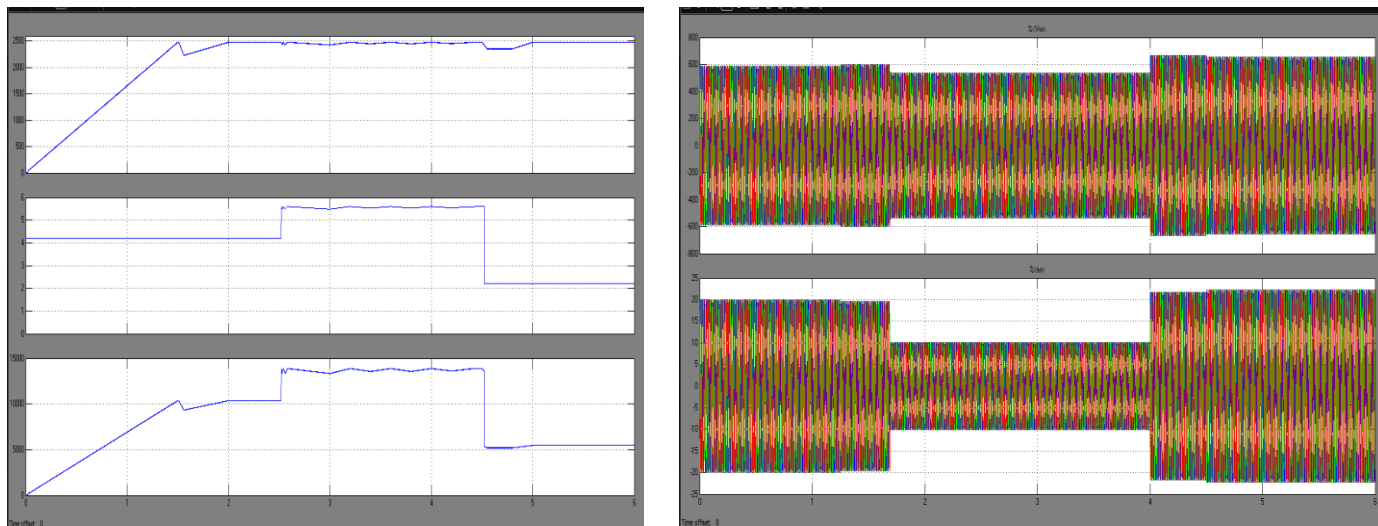


Fig. 12. Generated (a) voltage (b) current (c) power profile of the PV array under variable irradiance of the Sun.

Fig. 13. Instantaneous (a) voltage (b) current profile of the PMSG connected with WT

Figure.12 represents the voltage, current and power profiles for different irradiance of the sun. In the initial stage, the generated values are less because of the slow performance of IC based MPPT controller. The controller takes around 1.6 Sec to reach the maximum power around 10 kW due to 0.698 kW/m<sup>2</sup> solar irradiance. At 2.52 Sec the irradiance changes to the 0.928kW/m<sup>2</sup> and the PV array generates 13.9 kW. After 4.52 Sec the irradiance changes to 0.378 kW/m<sup>2</sup> and the PV array generates 5.8 kW electricity. Figure.13 represents the voltage and current profile of PMSG. The voltage almost remains constant but the current changes due to the change in wind speed.

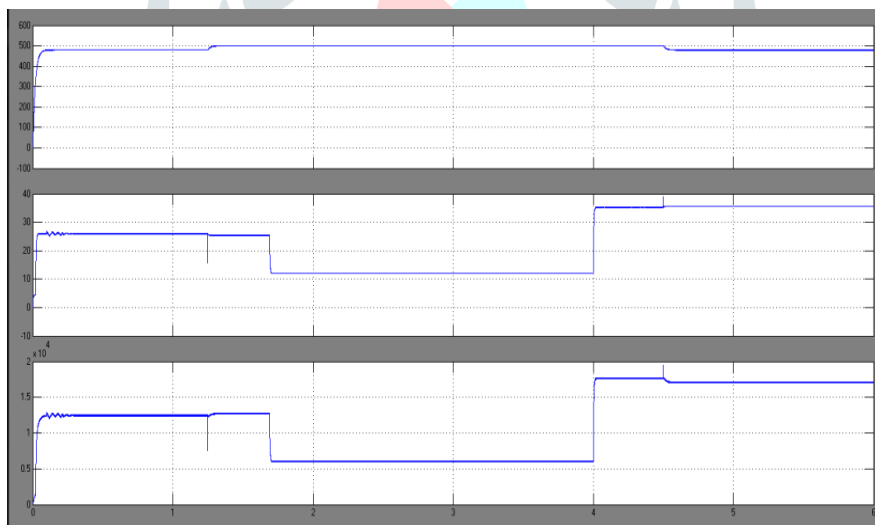


Fig.14.The rectified (a) voltage (b) current (c) power profile of the PMSG connected with WT.

The generated energy of PMSG is supplied to 3-phase rectifier which converts A.C to D.C, Figure represents the voltage, current and power profiles of the rectified output.

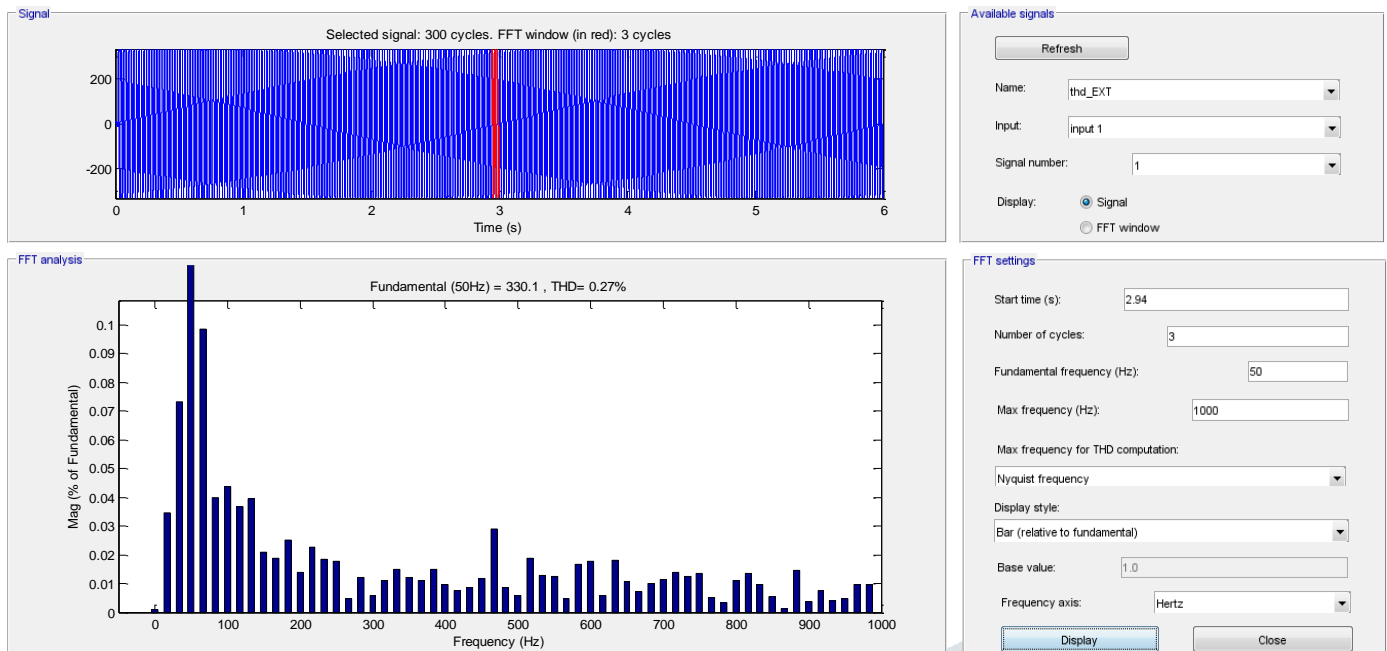


Fig.15.Harmonic spectrum of load voltage.

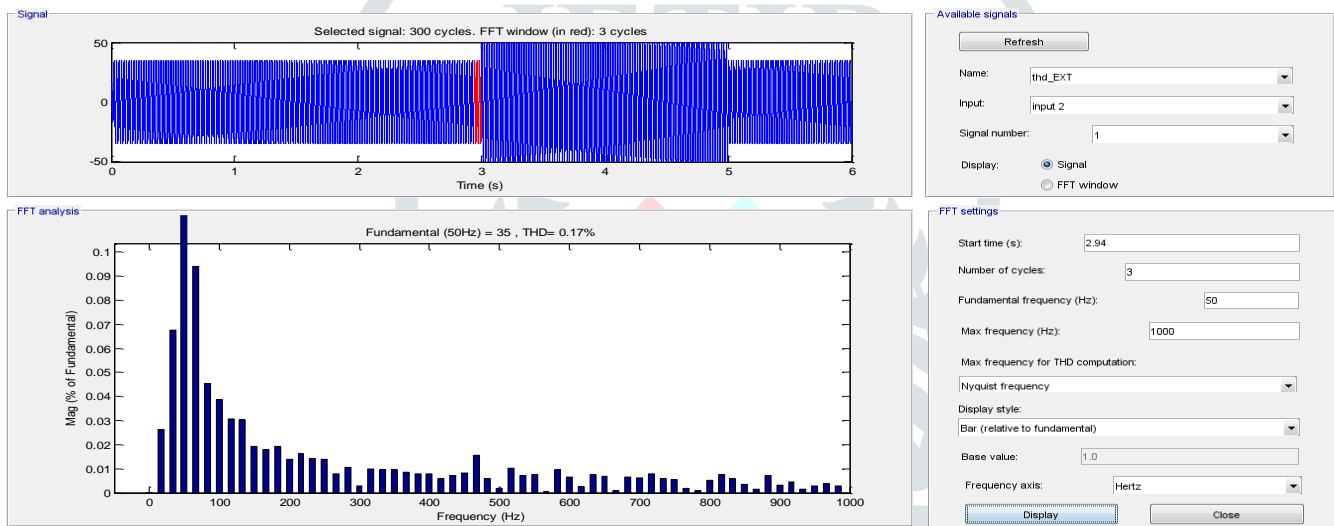


Fig.16.Harmonic spectrum of load current

Figure.15 & Figure.16 represents the harmonic spectrum of Load voltage and Load current using ANFIS Controller.

**V. CONCLUSION:**

In this Proposed a standalone hybrid power system using solar and wind energy is successfully modeled. Both the MPPT controller performance is satisfactory under variable irradiance and wind speed and maintains maximum power from the energy sources. The converter and the inverter unit has successfully maintains the power quality as per the standard. The charge controller for the hybrid power management performance is satisfactory. The hybrid battery management system maintains the energy flow to the load using different switches connected with the system. The different battery system maximizes the energy intake from the renewable energy sources and maintains reliable power to the consumer with the minimum battery capacity.

Controller		PI Controller	ANFIS
%THD	Load voltage	5.76%	0.27%
	Load current	5.46%	0.17%

**REFERENCES:**

[1] Arifujjaman, M., 2010. Modeling, simulation and control of grid connected Permanent Magnet Generator (PMG)-based small wind energy conversion system. IEEE Electr. Power Energy Conf. 2010, 1–6.

- [2] Ebrahimi, M.J., 2015. General overview of maximum power point tracking methods for photovoltaic power generation systems. *Int. Power Syst. Conf.*, 136–141
- [3] Jena, D., Rajendran, S., 2015. A review of estimation of effective wind speed based control of wind turbines. *Renew. Sustain. Energy Rev.* 43, 1046–1062.
- [4] Lee, K.J., Lee, J., Shin, D., Yoo, D., Kim, H., 2014. A novel grid synchronization PLL method based on adaptive low-pass notch filter for grid-connected PCS. *IEEE Trans. Industr. Electr.* 61 (1), 292–301.
- [5] Wu, Z., Dou, X., Chu, J., Hu, M., 2013. Operation and control of a direct-driven PMSGbased wind turbine system with an auxiliary parallel grid-side converter. *Energies* 6, 3405–3421.
- [6] Xiaodong, W., Shixu, H., Shirong, W., Yingming, L., Lixia, L., 2013. Multi-objective optimization torque control of wind turbine based on LQG optimal control. *25th Chinese Control Decision Conf. (CCDC)*, 405–408.
- [7] Zhihui, Ren, Zhongdong, Yin, Bao, W., 2009. Control Strategy and Simulation of Permanent Magnet Synchronous wind Power Generator. *Environment Technology*, pp. 568–571.
- [8] Zoua, C., Zhao, Q., Zhang, G., Xiong, B., 2016. Energy revolution: from a fossil energy era to a new energy era. *Natl. Gas Industry B.* 3 (1), 1–11.
- [9] Saw, L.H., Somasundaram, K.K., Ye, Y., Tay, A.A.O., 2014. Electro-thermal analysis of Lithium Iron Phosphate battery for electric vehicles. *J. Power Sources* 249, 231–238.
- [10] Rashid, M.H., 2007. *Power Electronics Handbook*. Elsevier, USA.

### Author's Profile:



**Mr. P. SHASHAVALI** Received his B.Tech Degree from the JNT University Hyderabad. He received Master of Technology degree from G. Pulla Reddy Engineering College Kurnool. Currently he is Pursuing Ph.D degree from JNT University Anantapur. Presently, he is working as Assistant Professor in the Department of Electrical and Electronics Engineering, S.K.University College of Engineering & Technology, S.K.University, Ananthapuramu-515 003, Andhra Pradesh, India. His research area of interest is Reliability concepts in Power Electronic Converters, Renewable Energy Sources and Facts Devices.



**Mr. N. RAJESH KUMAR GOWD** has graduated his B.Tech from St. John's College of Engg & Tech, Kurnool, A.P, India and M.Tech (EPE) from Bharath institute of Engineering and Technology Ibrahimpatnam, Hyderabad, T.S, India. Presently he is working as Assistant Professor in the Dept of EEE, Sri Krishnadevaraya University college of Engineering and Technology, Ananthapuramu - 515003, A.P, India. He has published 9 International Journals & 3 National conferences. His research areas of interest are Electrical Power System-Smart Grid, Reliability, Power electronics design.



**Mr. BUKKE HARINADHA NAYAK** has graduated his B.Tech from Sri Krishnadevaraya University college of Engineering and Technology Ananthapuramu, A.P. Currently he is pursuing M.Tech (Electrical Power Systems) from Sri Krishnadevaraya University college of Engineering and Technology, S.K.University, Ananthapuramu-515 003, A.P, India. His areas of interest are Power Systems and Renewable Energy Sources.